On Application of PHY Layer Abstraction Techniques in IEEE 802.11ac/ax WLANs

Roger Pierre Fabris Hoefel and *Oscar Bejarano*

***Abstract*—This paper investigates the application in IEEE 802.11ac/ax systems of the received bit information rate (RBIR) technique in order to estimate the effective signal-to-interference-plus-noise ratio used to abstract the physical layer (PHY) performance in system level simulations. The RBIR technique is evaluated based on simulation results of 802.11ac PHY operating over flat and spatial-correlated frequency selective single-user and multi-user MIMO channels. We have concluded that RBIR PHY abstraction methodology is accurate enough to provide first order insights on system level performance and design options with reduced computational complexity.**

Keywords: 802.11ac, 802.11ax, MIMO, OFDM, RBIR.

I. INTRODUCTION

The main target of the 2013 IEEE 802.11ac amendment [1] is to improve the physical layer (PHY) throughput (or link level throughput) of the 2009 IEEE 802.11n amendment[2], i.e.,the maximum theoretical throughput is increased from *600 Mbps*to *6.77 Gbps* in wireless local area networks (WLANs) based on the 802.11ac specification. Basically, PHY data rates improvements in 802.11ac WLANs have been achieved by operating with bandwidths (BW) of *20/40/80/80+80/160 MHz*; orthogonal frequency division multiplexing (OFDM) single-user (SU) multiple input multiple output (MIMO) with up *8* layers; quadrature amplitude modulation (QAM) schemes with cardinalities that range from *2* to *256* [3]. The optional implementation of downlink multi-user MIMO (DL MU-MIMO) allows improving the system throughput when the system is loaded with stations (STAs) that have a smaller number of antennas than the number antennas deployed at the access point (AP), i.e., a common scenario in corporative WLANs loaded with small form factor devices, such as smartphones and tablets [4].

The scarcity of "front-beach" spectrum below 6 GHz and the explosive demand of number of devices and traffic have driven intensive research and development (R&D) to cope with these challenges upon restrictions of capital expenditure/operational expenditure (CAPEX/OPEX). One short/medium term solution considered in the scope of 3GGP is the development of Long Term Evolution Unlicensed (LTE-U) specification to operate at the unlicensed 5 GHz band for traffic offloading [5].

In the scope of Wi-Fi community, the Task Group (TG) 802.11ax was created in March 2014 [6] to develop a new 802.11 amendment to face the following challenges: *(i)* exponential increase of traffic and number of devices in dense networks scenarios; *(ii)* competition of LTE-U; *(iii)* demands of telecom operators to offload traffic; *(iv)* desire of device vendors to offer better user experience urged in corporative and consumer electronic market segments; *(v)* pressure of chip set vendors to create a Wi-Fi market after the 802.11ac standard amendment. The Draft 1.0 of 802.11ax is expected to be approved 2016, while the Final Spec is forecasted to 2019.The IEEE 802.11ax amendment aims at increasing per area throughput efficiency in dense networks deployed in outdoor and indoor environments with major concerns about power consumption instead of focusing in per-link throughput in indoor networks as in the earlier 802.11 specifications.

The application of cross-layer techniques to design medium access control (MAC) and PHY protocols has driven the TGax to define a uniform set of PHY layer abstraction techniques in order to evaluate the performance of the different specification proposals considered in TG 802.11ax [7]. In section II, we contextualize the contributions of this paper to recent R&D activities that have been carried out in IEEE TG 802.11ax on the application of quality metric (QM) models for enabling system level simulations with affordable computational complexity. The remaining of this paper has the following layout: Section III describes the received bit information rate (RBIR) technique used to calculate the effective signal-to-interference-plus-noise ratio (ESINR) used to estimate the packet error rate (PER) without extensive PHY simulations for each channel realization. Section IV presents simulation results to validate the RBIR PHY abstraction technique in the context of 802.11ac/x WLANs over a set of realistic operational conditions. Finally, our conclusions are stated in Section V.

II. RELATED WORKS AND MAIN CONTRIBUTIONS

Research on application of PHY abstraction techniques for system level simulation were primarily carried out at the beginning of broadband cellular networks standardization process in 3GPP [8], 3GPP2 [9] and IEEE 802.16 Working Group (WG) [10]. Application of PHY abstraction techniques in Long Term Evolution (LTE) system level simulators can be found in [11-12].

The process of defining a methodology to PHY abstraction in 802.11 TGs [13] also occurred concomitantly with the activities developed at 3GPP and 802.16 WG [8-10]. However, WiFi semiconductor players only have demanded strong attention on this topic at the beginning of IEEE 802.11ax standardization process [7] due to the paradigm change from link level design to cross-layer optimization of PHY and MAC protocols that demands efficient design tools in order to evaluate the system performance over typical usage cases forecasted in ultra-dense networks deployments[14].

The technique of mapping the SINR observed at the OFDM MIMO detector output to the effective SINR (ESINR) scalar metric based on mutual information (MI) [15] is a strong

Roger Pierre Fabris Hoefel, Electrical Engineering Department, Federal University of Rio Grande do Sul (UFRGS), Porto Alegre, Rio Grande do Sul, Brazil. E-mail: roger.hoefel@ufrgs.br.

Oscar Bejarano, Electrical and Computer Engineering Department, Rice University, Houston, Texas, USA. E-mail: obejarano@rice.edu.

candidate to be chosen in TGax [7, 16] to implement PHY abstraction. For the best of our knowledge, public studies on this subject have been mainly restricted to TGax meetings. Reference [17] is one of few peer-to-peer review papers where the application of PHY abstraction techniques in wireless local area networks (WLANs) is investigated. However, this paper only shows simulation results based on the 802.11n amendment, assuming 2x2 SU-MIMO spatial multiplexing with *ideal channel state information* (CSI) at receiver side (Rx).

In this paper, we investigate the application of RBIR for ESINR mapping in 802.11ax system assuming *realistic synchronization and channel estimation* schemes over setups not widely investigated in TGax documents in the context of PHY abstraction, such as, the effects of the number of SU-MIMO spatial streams (SS) and DL MU-MIMO with block diagonalization (BD) pre-coding over spatial correlated and frequency selective TGn/ac MIMO channels.

The 802.11ax PHY is not defined yet. Therefore, we follow the same approach that has been used in the TGax, i.e., the simulation results are based on the 802.11ax amendment [7, 13-14]. A concise, but highly clear and instructive, description of main operational characteristics of IEEE 802.11ac PHY is presented in [18]. A description and validation of the IEEE 802.11ac simulator used in this paper is developed in [19].

Finally, we must reemphasize that the results shown in this paper assume *realistic* least square (LS) channel estimation scheme and time and frequency synchronization over spatial and frequency selective TGn/ac MIMO channel models. This is one of ***main differential aspects of this paper*** in relation to technical reports and presentations carried out in TGax [7, 13-14].

Table I– Basic parameters of IEEE 802.11ac simulator [19].

Parameter	Value	Parameter	Value
Carrier Frequency	5.25 GHz	MCS	0-9
Bandwidth	20 MHz, 40 MHz, 80 MHz	Number of Spatial Streams	1 to 8
GI Length	800 ns	Synchronization	Auto-Correlation
Modulation	BPSK, QPSK, 16-QAM, 64QAM, 256-QAM	MIMO Channel Estimation	Least Square
Binary Convolutional Code (BCC)	Code rate: r=1/2, r=2/3, r=3/4, r=5/6	Channel Decoder	Hard and Soft-Decision Viterbi Decoding

III. RBIR IN THE CONTEXT OF IEEE 802.11AC/AX

A. Effective SINR

The performance of MIMO OFDM systems depends on the statistics of the SINR measured at the MIMO detector output (i.e., the post-processing SINR).The application of quality metric (QM) techniques to evaluated the MIMO OFDM system performance with small complexity is founded on mapping the set of post-processing SINRs $\{SINR_{n,k},\ n=1,\cdots,N_{ss}, k=1,\cdots N_{sc}\}$ for all N_{sc} data subcarriers (SC) for each one of the N_{ss} spatial streams (SS) to an ESINR. This ESINR allows that the PER estimated over an OFDM MIMO additive white Gaussian noise (AWGN) channel be equivalent to that one estimated with full PHY simulation over the block fading channel realization where the ESINR was determined [15].

The general definition of the effective SINR mapping (ESM) for MIMO OFDM systems is given by [7]

$$SINR_{eff} = \alpha\Phi^{-1}\left(\frac{1}{N_{ss}}\frac{1}{N_{sc}}\sum_{n=1}^{N_{ss}}\sum_{k=1}^{N_{sc}}\Phi\left(\frac{SINR_{n,k}}{\beta}\right)\right), \quad (1)$$

where $SINR_{n,k}$ denotes the SINR at MIMO detector output at *k*th SC of the *n*th SS,$\Phi(.)$ is the ESM function, α and β are tuning factors. In this paper, we assume $\alpha=\beta=1$since in this case we can evaluate the minimum performance level of the RBIR PHY abstraction technique.

Assuming M-ary modulation with cardinality M, the received bit information rate (RBIR) metric uses an ESM function given by [15]

$$\Phi(\gamma) = E_{XY}\left\{log_2\frac{f(y/X,\gamma)}{\sum_{m=1}^{M}P(X)\cdot f(y/X,\gamma)}\right\}, \quad (2)$$

where X is a complex discrete random variable (r.v.) with probability distribution $P(X)$ that models the transmit symbols from the M-ary constellation, Y is a continuous r.v. that models the channel output with SINR equal to γ, and $f(y/X,\gamma)$ denotes the conditional probability density function (pdf) of the r.v Y measured at the AWGN channel output given the random variables X and γ.

Eq. (2) can be expanded to a numerical expression as follows

$$\Phi(\gamma_{n,k}) = log_2 M - \frac{1}{M}\sum_{i=1}^{M}E_U\left\{log_2\left(\frac{\sum_{j=1}^{M}exp\left[-\left|\sqrt{\gamma_{n,k}}\cdot(s_j-s_i)+U\right|^2\right]}{exp[-|U|^2]}\right)\right\}, \quad (3)$$

where $\gamma_{n,k}$ denotes the SINR measured at *k*th SC in the *n*th SS, s_k and s_m are constellation points with normalized energy and U is a circular symmetric complex Gaussian (CSCG) r.v. with zero mean and unitary variance [10].

B. MIMO AWGN CHANNEL

The MIMO AWGN channel model was proposed as comparison criteria for the PHY performance of the submitted proposals during the IEEE 802.11n standardization process [3, pp. 122].The unitary MIMO matrix H (cf. Eq. 4) is obtained taking the first N_{rx} x N_{tx} elements from the Fourier matrix with dimension $N = \max(N_{rx}, N_{tx})$, where $W = \exp(-j2\pi/N)$, N_{tx} and N_{rx} denote the number of transmit and receive antennas, respectively.

$$\mathbf{H}=\begin{bmatrix}1 & 1 & 1 & \cdots & 1\\ 1 & W^{1} & W^{2} & \cdots & W^{(N-1)}\\ 1 & W^{2} & W^{4} & \cdots & W^{2(N-1)}\\ \vdots & \vdots & \vdots & \ddots & \vdots\\ 1 & W^{(N-1)} & W^{(N-1)2} & \cdots & W^{(N-1)^2}\end{bmatrix}. \quad (4a)$$

The *m*th column vector at *k*th subcarrier $\mathbf{r_k}[\mathrm{m}] \in \mathbb{C}^{\mathrm{N_{rx}}}$ at the output of MIMO channel is given by

$$\mathbf{r_k}[\mathrm{m}] = \mathbf{H_k}[\mathrm{m}]\mathbf{x_k}[\mathrm{m}] + \mathbf{n_k}[\mathrm{m}], \quad (4b)$$

where $\boldsymbol{x}_{\mathrm{k}}[\mathrm{m}] \in \mathbb{C}^{\mathrm{N_{tx}}}$denotes the *m*th transmitted symbol at kth subcarrier and $\mathbf{H_k}[\mathrm{m}]$ is channel matrix observed at the receiver input at *m*th symbol and *k*th subcarrier. The additive noise is circular symmetric Gaussian r.v. with variance N_0, $\mathbf{n}\sim\mathcal{CN}\left(0, N_o\mathbf{I_{N_{rx}}}\right)$, where $\mathbf{I_{N_{rx}}}$ is a square identity matrix. Notice that for AWGN channel the MIMO channel matrix is the deterministic one given by (4a), which it is the same for each subcarrier. For TGan/ac MIMO channel models the stochastic MIMO channel matrix is determined according with the procedures described in [19].

C. Received Bit Information Rate over MIMO AWGN Channels

Fig.1a shows the RBIR as a function of the SNR for the 4x4 AWGN channel assuming LS channel estimation scheme and minimum mean squared error (MMSE) receiver. Assuming a SNR of *10 dB*, the RBIR is *1.0* and *1.97* for binary phase-shift keying (BPSK) and quaternary phase-shift keying (QPSK) modulation schemes, respectively. Notice that the maximum RBIR values for BPSK and QPSK are 1 and 2, respectively. Assuming the same SNR of *10 dB,* the RBIR is only *70%, 48%* and *37%* of its maximum value of *4* (16-QAM), *6* (64-QAM) and *8* (256-QAM), respectively.

Fig. 1b shows that non-ideal channel estimation decreases the RBIR directly proportional to the modulation cardinality. For instance, when perfect CSI is assumed a RBIR of 5 bits is obtained with a SNR of *17 dB* and *15 dB* for 64-QAM and 256-QAM, respectively. However, SNR of *20 dB* (64-QAM) and *18.5 dB* (256-QAM) are demanded when the realistic LS channel estimation scheme is assumed. Therefore, we can infer that power losses that range from *3* to *3.5 dB* occurs due to imperfect CSI over MIMO AWGN channels.

Extensive simulation results have shown that the PER over MIMO AWGN channels presents a negligible dependence on BW and number the antennas even when it is assumed MIMO AWGN channels with realistic synchronization, LS channel estimation scheme and MMSE MIMO detectors. Therefore, the results for MIMO AWGN channels can be expressed as function of signal-to-noise ratio (SNR) instead of SINR due to negligible multiple spatial stream interference. Finally, observe that the results shown in Fig. 1 also can be used to estimate the performance for other AWGN MIMO channel configurations (e.g., number of antennas, BW) due to the aforementioned remarks.

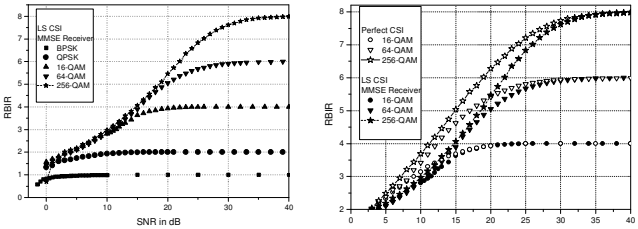

Figure 1. RBIR as function of SNR over AWGN channel: **(a)** Perfect CSI; **(b)** Perfect and LS CSI.

D. PER over AWGN Using PHY Layer Simulation

Tab. II, assuming an AWGN 2x2 MIMO channel, shows that our 802.11ac PHY simulation results present a close agreement with the PHY simulation results presented in [7], i.e., there is a first order consistence of the results shown in this paper. Notice that the results show in Tab. II assume perfect CSI and decorrelator receiver, i.e. the same assumptions used in [7].

Fig. 2 shows the MAC protocol data unit (MPDU) PER as a function of SINR over a MIMO AWGN channel with BW of *20 MHz*. The receiver implements LS channel estimation and MMSE receiver with soft-decision Viterbi decoding. An MPDU payload of 1500 bytes is assumed. Finally, notice that for the AWGN channel the ESNR and SNR have the same logical meaning.

Table II - SNR in dB to obtain a PER of 1%. AWGN 2x2. MPDU sizes of 250/500/1000/1000 bytes for QPSK (MCS1), MCS4 (16-QAM) and MCS6 (64-QAM) and MCS8 (256-QAM). Soft-decision Viterbi decoding.

	MCS1	MCS4	MCS6	MCS8
Simulation Perfect CSI	3.5 dB	12.8 dB	18.8 dB	24.3 dB
Ref. [7] Perfect CSI	4.0 dB	13.0 dB	18.5 dB	24.5 dB

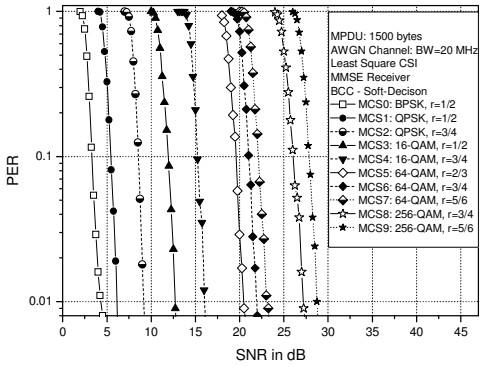

Figure 2. PER vs. SNR in dB for LS channel estimation.

Fig. 3 shows that a realistic receiver with LS channel and MMSE detection estimation presents power losses between 2.5 (MCS2) and 3 dB (MCS8) in relation to an hypothetical system with perfect CSI and ideal decorrelator receiver, i.e., these results are consistent with the losses in the RBIR due to imperfect CSI at Rx side shown in Fig. 1b.

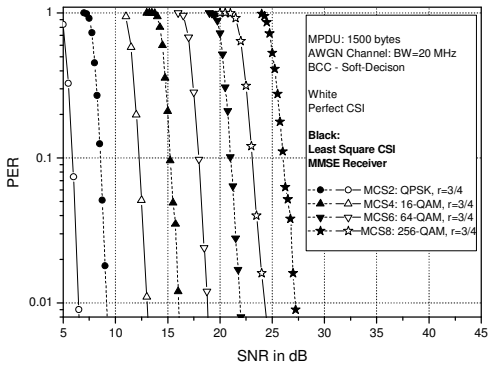

Figure 3. Effects of imperfect channel estimation on the PER.

E. PER Using PHY Layer Abstraction

The algorithm based on RBIR and ESINR to estimate the PER in MIMO OFDM systems is summarized as follows:

Step 1. Determine the $SINR_{n,k}$ at the output of MIMO detector for all SSs ($n=1,...,N_{ss}$) and SCs ($k=1,...,N_{sc}$). These values of SINR must be obtained for the modulation code scheme (MCS) being evaluated in the 802.11ac/ax simulator that consistently abstract the details of PHY layer. Notice that the $SINR_{n,k}$ depends on both the modulation scheme and code rate specified for each MCS.

Step 2. Use the mapping function specified in (3), with the appropriate modulation constellation and the *SINR* measured for all SSs and SCs ($\gamma_{n,k}$), in order to obtain the set $\{\Phi(\gamma_{n,k}), n = 1, \cdots, N_{ss}, k = 1, \cdots N_{sc}\}$.

Step 3. Use *(5)* to obtain the *RBIR* using the set of SINRs specified at step (2).

$$RBIR = \frac{1}{N_{ss}}\frac{1}{N_{sc}}\sum_{n=1}^{N_{ss}}\sum_{k=1}^{N_{sc}}\Phi(SINR_{n,k}). \quad (5)$$

Step 4. A table look up procedure is used to map the RBIR to the ESINR. In this paper, we use the data shown in Fig. 1. Notice that the LS channel estimation schemed and realistic synchronization is assumed, instead of the oversimplified *ideal channel estimation and synchronization* assumptions postulated in [7, 16].

Step 5. Use the ESINR calculated at step (4) to estimate the PER probability using a table look up procedure to perform the mapping from ESNR to PER. These tables are obtained from full PHY layer simulation over the AWGN channel. In this paper, otherwise noticed, we use the results shown Fig. 3, which depend upon MPDU length, channel estimation scheme and receiver type.

IV. Evaluation of RBIR in 802.11ac/ax WLANs

A. Histogram of RBIR and PER

Figures 4a and 4b, using *5000* different channel realizations, show the histogram of RBIR and frequency of PER as a function of RBIR, respectively, when a MPDU payload of *1500 bytes* is transmitted using MCS3 (*16-QAM, BCC with r=1/2*) over the TGac B 4x4 channel with a SNR of *34 dB*. The residential TGac B MIMO channel model is a spatial-correlated low-frequency selective with two clusters, maximum excess delay of *80 ns* and root mean square (rms) delay spread of *15 ns* [3, pp. 38].The RBIR has an average value of*3.39.* If the first moment (average) of the RBIR is used in Fig. 1, then a SNR of *13 dB* is obtained. Using this value in Fig. 2, a negligible PER is estimated (i.e., much smaller than *0.01*). However, PHY layer simulation results show a PER of *0.16* when the SNR is equal to *34 dB*. This mismatching occurs because in wireless systems operating over MIMO multipath fading channels, the events with low SINR are the ones that generate outage on the system performance and, therefore, use the average RBIR to estimate the PER in MIMO channels is not the correct procedure

On the other hand, Fig. 2 shows that a PER of *0.16* occurs when the SNR is equal to *11.75 dB* and Fig. 1 shows that this value corresponds to a RBIR of *3.2*. Finally, using Figures 4a and 4b, an estimated PER of *0.19 (91/482)* is observed for RBIR equal to *3.2*, i.e., close to the measured PER of *0.16* obtained with full PHY layer simulation.

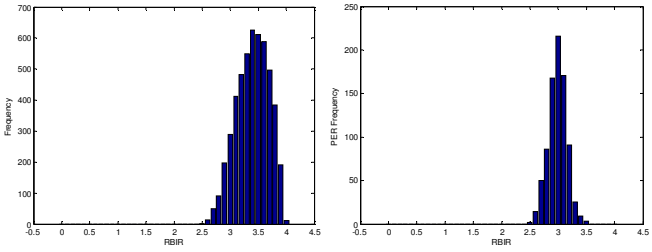

Figure 4a. Histogram of RBIR for a TGac B 4x4channelwith SNR of 34 dB.
Figure 4b. Frequency of PER as a function of RBIR.

Finally, based on the reasoning carried out in this subsection, the methodology to validate the RBIR as viable technique to obtain the PER in IEEE 802.11ac/ax systems is accomplish by comparing the PER measured using the histograms of RBIR and histograms of PER as a function of RBIR (which are obtained using complete PHY simulation) with the PER estimated using the PHY layer abstraction using the algorithm described in Section III.

B. Application of ESINR for PER Estimation: SU-MIMO

Fig. 5 shows the PER as a function of ESINR, where the TGac B 4x4 MIMO channel, *realistic synchronization and channel estimation schemes* and linear MMSE MIMO receiver is assumed. These results allow to infer that the abstraction of PHY using the ESINR mapping based on the RBIR technique is an effective technique since a difference less than *1 dB* between the PER obtained using the abstraction of PHY (i.e., results show by bold geometric figures) and PER obtained with link level simulation (i.e., results show by white geometric figures) is observed.Technical reports have shown a mismatching of less than 0.6 dB when perfect synchronization and channel estimation schemes are assumed over MIMO 2x2 TGac B and D channels [7, 14]. Finally, notice that the use of tuning at Eq. (1) can improve the matching between the simulation results with and without PHY abstraction techniques.

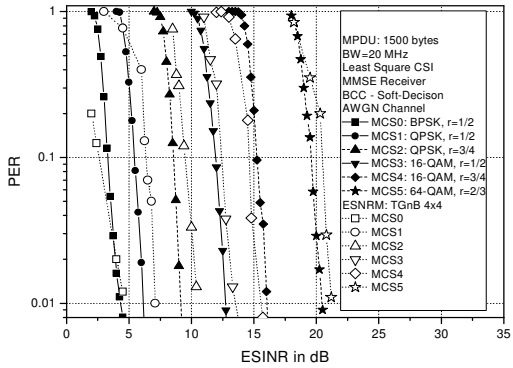

Figure 5. Comparison between the PER obtained using the equivalent AWGN channel (white geometric figures) and the PER for TGac B 4x4 channel using ESINR based on RBIR technique. MPDU payload of 1500 bytes.

The performance of BCC with soft-decision Viterbi decoding depends on the MPDU packet length. Therefore, Fig. 6 assumes a MPDU payload of *1000 bytes*, instead of *1500 bytes* assumed in earlier figures, in order to evaluate the performance of RBIR technique with different packet lengths. Fig 6 shows as bold geometric figures the PER as function of SNR over TGac B 2x2, TGac D 2x2 and TGac D 4x4 channels, while the white geometric figures correspond to the PER as a function of ESINR is depicted. The typical office TGac D channel is a spatial-correlated and highly frequency selective channel model with three clusters, maximum excess delay of *390 ns* and rms delay spread of *50 ns* [3, pp. 38]. Notice that in the full PHY simulation the results are expressed as function of SNR, while it is necessary to use the ESINR when the PHY layer abstractions are used. The following setup is assumed: BW of 20 MHz; MCS3 (16-QAM, BCC with r=1/2); LS channel estimation; MMSE receiver, soft-decision Viterbi decoding. Fundamentally, these results ratify, using a distinct MPDU payload, that the techniques to obtain the ESNR using the RBIR paradigm allow estimating the PER with the adequate precision for system level simulation since there is a mismatching of less than *1 dB* between the estimated ESINR over the MIMO channels and the ESINR used to estimate the PER over the AWGN channel. Observe that an ESINR of *12.5 dB* is demanded to obtain a PER of 1% over the AWGN channel. For the TGac D 2x2 channel, a SNR of *28 dB* is necessary to obtain this ESINR of 12.5 dB, while an intangible SNR of *44 dB* is need when the TGac D 4x4 is simulated.

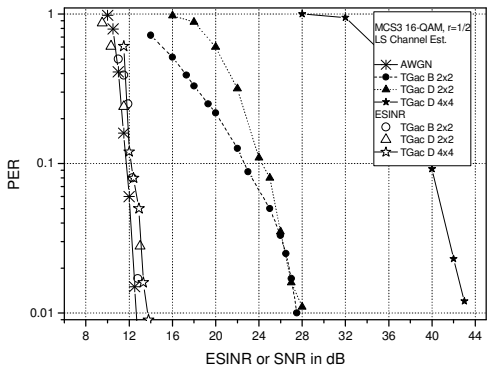

Figure 6. Comparison between the PER obtained as a function of SNR (left curves) with the PER obtained as function of ESNR (right curves). BW of 20 MHz. MPDU payload of 1000 bytes.

B. Application of ESINR for PER Estimation: MU-MIMO

The description of MU-MIMO channel models, block diagonalization precoding scheme and MMSE MIMO detector used in this paper can be found in [19].

Fig. 7 shows the PER as a function of SNR and ESINR for 802.11ac systems operating over TGac D MU-MIMO channels. The following configuration is assumed: 4x2x2 (4 transmit antennas, 2 receive antennas per STA, 2 STAs); 2 SSs per STA; block diagonalization (BD) pre-coding; realistic synchronization and LS channel estimation, MMSE MIMO detector, soft-decision Viterbi decoding, BW of 80 MHz and MPDU payload of 1500 bytes. The bold geometric figures of Fig. 7 show the PER as function of SNR for MCS0 to MCS3, while the white ones show the PER as a function of ESINR is depicted. These results also show a good matching between the PER obtained using PHY simulation and the PER obtained with RBIR abstraction technique for MCS0 and MCS3. However, there is a mismatch of approximately 2 dB for MCS2 and MCS3. Therefore, comparing these results with those ones shown for SU-MIMO system (cf. Figs. 5 and 6), we have concluded that for MU-MIMO is necessary additional procedures in order to tuning Eq. (1) if greater accuracy is demanded.

VII. CONCLUSIONS

First, we describe the motivations that drive R&D on the application of PHY abstraction techniques for system level simulation in the framework of IEEE 802.11ax specification. Second, we develop in great detail the application of the received bit information rate technique used to calculate the ESINR as well as the mapping of ESINR to PER. Third, we show that our simulation results present a good agreement with those ones publicized by the TG 802.11ax, where perfect synchronization and channel estimation are assumed. Next, we verify that realistic channel estimation and synchronization schemes present a power loss that range from *3* to 3.5 dB due to imperfect synchronization and CSI even over MIMO AWGN channels. Finally, we have concluded that the PHY layer abstraction technique based on RIBR is adequate for providing insights on system level performance and design options with low computational burden.

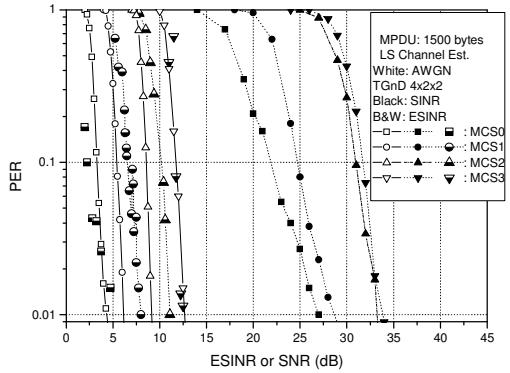

Figure 7. Comparison between the PER obtained as a function of SNR (left curves) with the PER obtained as function of ESNR (right curves).

REFERENCES

[1] Wireless LAN Medium Access Control and Physical Layer Specifications, Amendment 5: Enhancement for Very High Throughput for Operations in Bands below 6 GHz. IEEE P802.11ac, Dec. 2013.

[2] Wireless LAN Medium Access Control and Physical Layer Specifications, Amendment 4: Enhancement for Higher Throughput. IEEE Std 802.11n-2009, June 2009.

[3] E. Perahia and R. Stacey, *Next Generation Wireless LANS*: *802.11n and 802.11ac.*2th ed. Cambridge: Cambridge University Press, 2013.

[4] O. Bejarano, E. W. Knightly and M. Park. "IEEE 802.11ac: from channelization to multi-user MIMO,"*IEEE Communications Magazine, vol.* 51, no. 10, pp. 84-90, Oct. 2013.

[5] F. M. Abinader et. al. "Enabling the coexistance of LTE and Wi-Fi in unlicensed bands", *IEEE Communications Magazine, vol.* 52, no. 11, pp. 54-61, Nov. 2014.

[6] D-J. Deng, K-C. Cheng and R-S. Cheng. "IEEE 802.11ax: next generation wireless local area networks," *in 10th 2014 International Conference on Heterogeneous Networking for Quality, Reliability, Security and Robustness (QShine),* 2014.

[7] IEEE 802.11-14/0527-r1*, "PHY Layer Abstractions for TGax System Level Simulations,"* May 2014.

[8] 3GPP TSG-RAN-1 Meeting #35*,* R1-03-1298*, "Effective SIR Computation for OFDM System-Level Simulations*", Nov. 2003.

[9] 3GPP2-C30-20030429-010, "*Effective-SNR Mapping for Modeling Frame Error Rates in Multiple-State Channels*", Nov. 2003.

[10] IEEE 802.16m-08/004r5, *"IEEE 802.16m Evaluation Methodology Document",* 2009.

[11] R. Santos, W. Freitas , E. Stancanelli and F. Cavalcanti, "Link-to-system level interface solutions in multistate channels for 3GPP LTE wireless system," *in XXV Brazilian Symposium of Telecommunications*, 2007.

[12] J. C. Ikuno., M. Wrulich, M. Rupp, "System level simulation of LTE networks," *IEEE 71th Vehicular Technology Conference,* Ottawa, 2010.

[13] IEEE 802.11-04/0174r1, "*PHY Abstraction for System Simulation,"*2004.

[14] IEEE 802.11-13/1131r0, "*PHY Abstraction for HEW System Level Simulation",* Sept. 2013.

[15] L. Wan, S. Tsai and M. Almgren, "A fading-insensitive metric for unified link quality model," *in IEEE Wireless Network Conference 2006 (WCNC 2006),* April 2006.

[16]IEEE 802.11-14/08111r2, "Overview on RBIR-based PHY Abstraction", July 2014

[17] J. Wu, Z. Yin, J. Zhang and W. Heng, "Physical layer abstraction algorithms research for 802.11n and LTE downlink," *International Symposium on Signals, Systems and Electronics (ISSSE 2010),* Nanjing, China, 2010.

[18] D. Nojima, L. Lanante Jr., Y. Nagao, M. Kurosaki and H. Ochi, "Performance evaluation for multi-user MIMO IEEE 802.11ac wireless LAN system," in *14th International Conference on Advanced Communication Technology,* Feb. 2012.

[19] R. P. F. Hoefel. "Multi-User OFDM MIMO in IEEE 802.11ac WLAN: a simulation framework to analysis and synthesis", in *IEEE Latin America Transactions,* vol.13, no. 2, pp. 540-545, Feb.. 2015